BOREAL ENVIRONMENT RESEARCH 29: 35–52
ISSN 1797-2469 (online)

Helsinki 22 January 2024

Over 20 years of observations in the boreal forest reveal a decreasing trend of atmospheric new particle formation

Xinyang Li[1)], Haiyan Li[2)α], Lei Yao[3)α], Dominik Stolzenburg[1)4)], Nina Sarnela[1)], Lejish Vettikkat[5)], Robin Wollesen de Jonge[6)], Rima Baalbaki[1)], Helmi Uusitalo[1)], Jenni Kontkanen[1)], Katrianne Lehtipalo[1)7)], Kaspar R. Daellenbach[1)8)], Tuija Jokinen[1)9)], Juho Aalto[1)10)], Petri Keronen[1)], Siegfried Schobesberger[5)], Tuomo Nieminen[1)], Tuukka Petäjä[1)], Veli-Matti Kerminen[1)], Federico Bianchi[1)], Markku Kulmala[1)11)12)*] and Lubna Dada[1)8)*]

[1)] *Institute for Atmospheric and Earth System Research/Physics, Faculty of Science, University of Helsinki, Finland*
[2)] *School of Civil and Environmental Engineering, Harbin Institute of Technology, Shenzhen, 518055, China*
[3)] *Shanghai Key Laboratory of Atmospheric Particle Pollution and Prevention (LAP3), Department of Environmental Science and Engineering, Fudan University, Shanghai 200438, China*
[4)] *Institute for Materials Chemistry, TU Wien, 1060 Vienna, Austria*
[5)] *Department of Technical Physics, University of Eastern Finland, Kuopio, 70211, Finland*
[6)] *Department of Physics, Lund University, Professorsgatan 1, Lund, SE-22363, Sweden*
[7)] *Atmospheric Composition Research, Finnish Meteorological Institute, Helsinki, Finland*
[8)] *Laboratory of Atmospheric Chemistry, Paul Scherrer Institute, Villigen, 5232, Switzerland*
[9)] *Climate & Atmosphere Research Centre (CARE-C), The Cyprus Institute, P.O. Box 27456, Nicosia, CY-1645, Cyprus*
[10)] *Institute for Atmospheric and Earth System Research/Forest Sciences, Faculty of Agriculture and Forestry, University of Helsinki, Finland*
[11)] *Joint International Research Laboratory of Atmospheric and Earth System Sciences, School of Atmospheric Sciences, Nanjing University, Nanjing, China*
[12)] *Aerosol and Haze Laboratory, Beijing Advanced Innovation Center for Soft Matter Sciences and Engineering, Beijing University of Chemical Technology (BUCT), Beijing, China*
[α] *The second and third authors contributed equally to this work*
**corresponding authors' e-mail: lubna.dada@helsinki.fi; markku.kulmala@helsinki.fi*

Received 27 Sep. 2023, final version received 2 Nov. 2023, accepted 8 Nov. 2023

Li X., Li H., Yao L., Stolzenburg D., Sarnela N., Vettikkat L., de Jonge R.W., Baalbaki R., Uusitalo H., Kontkanen J., Lehtipalo K., Daellenback K.R., Jokinen T., Aalto J., Keronen P., Schobesberger S., Nieminen T., Petäjä T., Kerminen V.-M., Bianchi F., Kulmala M. & Dada L. 2024: Over 20 years of observations in the boreal forest reveal a decreasing trend of atmospheric new particle formation. *Boreal Env. Res.* 29: 25–52.

New particle formation (NPF) events substantially contribute to the number concentration of atmospheric particles and cloud condensation nuclei (CCN) which can further influence radiative balance and Earth's climate. Many short-term studies have found that sulfuric acid (H_2SO_4) and highly oxygenated organic molecules (HOM) are critical compounds in the early steps of NPF. However, it is not fully understood how NPF intensity and frequency respond to global warming and declining anthropogenic sulfur dioxide (SO_2) emissions,

Editor in charge of this article: Antti Arola

affecting HOM and H_2SO_4 formation, respectively. Here, we report the results of long-term (over 20 years) datasets collected at the Station for Measuring Ecosystem-Atmosphere Relations (SMEAR) II (Hyytiälä, Finland). Owing to the significant contribution of HOM in the initial and subsequent particle formation and growth, we have derived a HOM proxy for conducting the long-term trend analysis. Measurement results together with modelled proxies reveal the declining trends of SO_2, H_2SO_4, Condensation Sink (CS), NPF frequency and particle formation rate (J_3) along with increasing trends of monoterpenes and HOM.

Introduction

Atmospheric aerosol particles influence the Earth's radiative balance by scattering and absorbing solar radiation and acting as cloud condensation nuclei (CCN) (Charlson *et al.* 1992, Rap *et al.* 2013). New particle formation (NPF) is the dominant source of atmospheric aerosol particles in terms of their number concentrations (Kulmala *et al.* 2004a, Spracklen *et al.* 2010, Dunne *et al.* 2016), and it is thought to produce almost half of the global CCN in the atmospheric boundary layer as predicted from models (Merikanto *et al.* 2009, Gordon *et al.* 2017). The more recent studies revealed that even more than half of the global CCN are produced from NPF processes (Junninen *et al.* 2022, Kulmala *et al.* 2022a). The formation of particles is largely controlled by atmospheric precursor concentrations, pre-existing particles, and environmental conditions (Kulmala 2003, Kulmala *et al.* 2007, Clarke *et al.* 2013, Tröstl *et al.* 2016, Kerminen *et al.* 2018). As natural emissions (e.g., biogenic volatile organic compounds) are increasing in response to global warming while anthropogenic emissions are declining due to mitigation efforts (Wiedinmyer *et al.* 2006, Rogelj *et al.* 2014), it is essential to investigate the long-term changes of NPF to better understand the formation mechanisms of new particles and further improve the performance of climate models.

Atmospheric NPF events, including nucleation and subsequent growth, have been observed to occur in various locations worldwide (Kerminen *et al.* 2018, Chu *et al.* 2019). Sulfuric acid (H_2SO_4), mainly originating from atmospheric oxidation of sulfur dioxide (SO_2), is considered as a key component in atmospheric new particle formation (Kulmala *et al.* 2004b, Sihto *et al.* 2006, Sipilä *et al.* 2010). However, sulfuric acid alone or together with water cannot fully explain the observed formation and growth rates of new particles in ambient air (Weber *et al.* 1996, Spracklen *et al.* 2010). Thus, other atmospheric molecules are expected to participate in NPF in addition to sulfuric acid and water. Enhanced nucleation rates have been observed in the presence of additional species such as ammonia, amines and oxidized organic compounds (Coffman and Hegg 1995, Zhang *et al.* 2004, Kirkby *et al.* 2011, Almeida *et al.* 2013, Kulmala *et al.* 2013, Riccobono *et al.* 2014, Lehtipalo *et al.* 2018, Yao *et al.* 2018, Yan *et al.* 2021). After the initial step of cluster formation, condensing organic vapors give a significant, and often dominant, contribution to subsequent particle growth, especially in a boreal forest environment (Kulmala *et al.* 1998, Kulmala *et al.* 2004b, Kulmala *et al.* 2004c, Riipinen *et al.* 2012, Ehn *et al.* 2014, Mohr *et al.* 2019, Stolzenburg *et al.* 2023). These organic vapors are abundant in the continental boundary layer and are mainly formed through the oxidation of volatile organic compounds (VOCs) by ozone, hydroxyl radicals, and nitrate radicals (Ehn *et al.* 2014, Bianchi *et al.* 2019). Some of the organic vapors, especially highly oxygenated organic molecules (HOM), that are formed mainly via auto-oxidation of peroxyl radicals (RO_2), are also capable of initiating particle formation in certain conditions (Kulmala *et al.* 2013, Rose *et al.* 2018, Bianchi *et al.* 2019).

The increased temperatures, associated with global warming, especially over the northern mid and high latitudes are expected to accelerate the growth of trees and boost the emission rate of VOCs especially in boreal forest environments where vegetation is dense (Lathière *et al.* 2005, Peñuelas and Staudt 2010, Valolahti *et al.* 2015; Liu *et al.* 2019, Wang *et al.* 2023). Among the biogenic emissions, monoterpenes are the main group of VOCs present in the boreal forest envi-

ronment (Lindfors *et al.* 2000, Eerdekens *et al.* 2009, Hakola *et al.* 2012), although more recent studies have also highlighted the potential importance of sesquiterpenes to atmospheric chemistry (Hellén *et al.* 2018; Dada *et al.* 2023a). Aside from the rising global temperatures, environmental stressors such as heat waves, droughts, and insect infestation also strongly affect the behavior of plants. Studies show that more than 40% of forest trees in Europe are under stress (Zhao *et al.* 2017), so that they are likely to enhance VOC emissions and alter their chemical compositions in the long run (Holopainen, 2011, Holopainen *et al.* 2018, Bussotti and Pollastrini, 2021). In the case of the boreal forest, on the one hand, the dominating effect of increased temperatures results in a substantial increase in biogenic VOC emissions. The latter may enhance the production of HOM and thereby promote the formation and growth of new particles. This suggests potentially significant feedback between plant emissions and climate. On the other hand, anthropogenic pollutant emissions are declining due to the efforts to improve air quality and mitigate climate change (Rogelj *et al.* 2014). In Europe, emissions of non-methane anthropogenic VOCs decreased by more than a half since 1990, while SO_2 emissions have decreased by 91% from 1990 to 2017 (EEA 2019). The significant decline in SO_2 emissions may have led to weaker production of sulfuric acid, which might affect the occurrence and intensity of new particle formation events. Despite the changes in VOC and SO_2 emissions, the long-term trends of sulfuric acid, HOM and their relations with new particle formation rates are poorly understood at present due to lack of long-term, direct measurements.

Here, we use more than 20 years of datasets measured at the Station for Measuring Ecosystem-Atmosphere Relations (SMEAR) II (Hyytiälä, Finland) from 1996 to 2019 to explore the long-term trends of ambient temperature, SO_2, NPF frequency, growth rates and particle formation rate at 3 nm (J_3). For assessing the contribution of vegetation to new particle formation, we built a novel proxy to estimate HOM concentrations. In conjunction with the established parametrizations for sulfuric acid and monoterpenes, as well as newly developed parametrizations for HOM, can we estimate their concentrations and long-term trends. Based on these long-term trends, the relationship between NPF and its main precursors (i.e., sulfuric acid and HOM) was also probed.

Material and methods

Measurement site

Data used in this study were collected from the Station for Measuring Ecosystem-Atmosphere Relations (SMEAR-II) station from 1996–2019. The station locates in Hyytiälä, southern Finland (61°51′N, 24°17′E, 181 m a.s.l.). The surrounding pine and spruce forest homogeneously extend to the north and northeast. The largest city nearby is Tampere, located about 60 km to the southwest. Overall, the station represents a typical rural and background boreal forest site. The station is equipped with continuous and comprehensive measurements of the interactions between the forest ecosystem and the atmosphere. A detailed description of the station can be found in (Hari and Kulmala 2005).

Instrumentation

Sulfuric acid and HOM were measured from 2016 to 2019 using a Chemical Ionization Atmospheric Pressure interface Time of Flight mass spectrometer (CI-APi-TOF, Aerodyne Research Inc., USA) using nitrate anions as the reagent ion. The detailed information of the instrument's working principle has been described in previous studies (Jokinen *et al.* 2012, Ehn *et al.* 2014, Yao *et al.* 2018). The CI-APi-TOF has been calibrated twice per year using sulfuric acid as described in Kürten *et al.* (2012).

Monoterpenes were measured from 2010 to 2019 using a proton-transfer-reaction mass spectrometer (PTR-MS, Ionicon Analytik Inc., Austria) equipped with a quadrupole mass analyzer. The detailed description of the instrument's working principle can be found in previous studies (Rinne *et al.* 2005, Taipale *et al.* 2008, Kolari *et al.* 2012). The PTR-MS was calibrated weekly using pre-mixed VOC gas standards to maintain

accuracy and sensitivity. The calibration method was documented by Taipale *et al*. (2008).

Nitrogen monoxides (NO) were measured from 1996 to 2019 using a chemiluminescence analyzer (TEI 42 CTL, Thermo Fisher Scientific, MA, USA). Nitrogen oxides (NO_x) were measured from 1996 to 2019 using a chemiluminescence analyzer with heated metal (Mb) converter (TEI 42 CTL; Thermo Fisher Scientific, MA, USA). We subtracted NO_2 concentration from the difference between NO_x and NO concentrations, as NO_x is a collective term referring to nitrogen monoxide (NO) and nitrogen dioxide (NO_2).

Particle number size distributions were measured by a differential mobility particle sizer (DMPS) which consists of a 2mCi Krypton-85 beta source neutralizer, a DMA (Differential Mobility Analyzer) and a CPC (Condensation Particle Counter) (Aalto *et al.* 2001, Dal Maso *et al.* 2005). The DMPS system covered the size range from 3 to 500 nm before 2004 and after that from 3 to 1000 nm (Aalto *et al.* 2001; Nieminen *et al.* 2014). A Neutral cluster and Air Ion Spectrometer (NAIS) (Airel Ltd., Estonia) was also deployed to measure the number size distribution of neutral and charged aerosol particles and clusters in the size ranges of 2–40 nm and 0.8–40 nm, respectively (Mirme and Mirme, 2013). The measurements were conducted between 2006 and 2020 excluding the year 2008.

The SO_2 mixing ratios were recorded by two UV-fluorescence analyzers (Thermo Scientific, Model 43C-TLE from 1996 to 2012 and Model 43i-TLE after 2012). The O_3 concentration was measured with a UV light absorption analyzer (Thermo Scientific, Model TEI 49C). Global radiation (0.30–4.8 μm) and air temperature were recorded by pyranometers and 4-wire PT-100 sensors. The UVB intensity was measured with an UVB radiometer (Solar Light SL501A).

Theory for proxy calculations

Sulfuric acid proxy

The sulfuric acid proxy was obtained by considering its source and sink terms in the boreal forest environment as discussed in Dada *et al*. (2020). The formation of H_2SO_4 in the gas phase could be explained by the oxidation of SO_2 by the hydroxyl radical (OH) and the stabilized Criegee Intermediates (sCIs) while its sinks comprised the condensation of H_2SO_4 onto pre-existing particles, known as condensation sink (CS), as well as its loss to cluster/particle formation (Dada *et al.* 2020). The details of CS calculation can be found in Kulmala *et al.* (2012). Since OH concentrations are difficult to measure, a commonly used method is to implement global radiation as an OH proxy (Petäjä *et al.* 2009). A monoterpene (MT) proxy was used to simulate alkene concentrations at the SMEAR II station (Kontkanen *et al.* 2016) to account for the H_2SO_4 produced by sCIs. Altogether, the H_2SO_4 proxy concentration can be calculated as:

$$[H_2SO_4] = -\frac{CS}{2k_3} + \sqrt{\left(\frac{CS}{2k_3}\right)^2 + \frac{[SO_2]}{k_3}} \sqrt{\begin{matrix}(k_1\text{GlobRad} \\ +k_2[O_3][MT])\end{matrix}} \quad . \quad (1)$$

The fitting parameters k_1, k_2 and k_3 were obtained by fitting H_2SO_4 proxy concentrations to measured H_2SO_4 concentrations by Dada *et al*. (2020) were implemented in the above equation. Figure S1 (found in Supplementary Information) illustrates the validation of the developed sulfuric acid proxy by the inter-comparisons with observational data in earlier studies from the period 2016 to 2019, and the estimated $[H_2SO_4]$ displayed a good correlation with the measured H_2SO_4 concentration (r = 0.6), as well as the seasonal comparisons in Figure S2 (found in the Supplementary Information).

Monoterpene proxy

The monoterpene (MT) measurements were only available from 2010–2019. To obtain a long-term picture of MT variation before 2010, a MT proxy was determined based on the method by Kontkanen *et al.* (2016). A temperature-dependent MT emission function, developed by Tarvainen *et al.* (2005) has been found to correlate well with the MT emission in Hyytiälä via:

$$E = \alpha \times \exp(\beta\,(T - T_s)), \qquad (2)$$

where T is the temperature and T_s denotes the temperature at standard conditions (T_s = 303.15K; Tarvainen *et al.,* 2005, Lappalainen *et al.* 2009). Thus, in this work, a sole temperature-dependent emission function of MT was used as the only source term. The fitting parameters α and β were acquired from Kontkanen *et al.* (2016).

MT are mainly oxidized by ozone, OH and NO_3. However, neither OH nor NO_3 are directly measured at SMEAR II. Thus, the equivalent OH proxy and NO_3 proxy from Petäjä *et al.* (2009) and Peräkylä *et al.* (2014), respectively, were applied (see details in the next section).

The diluting effect of varying mixing layer height (*MLH*) and wind speed (*ws*) was combined with the MT source and sink terms to yield the MT proxy concentrations:

$$[MT]_{\text{proxy}} = \frac{a \cdot \exp(b(T - T_s))}{k_{\text{OH+MT}}[OH] + k_{\text{O}_3\text{+MT}}} \left(\frac{1}{[O_3] + k_{\text{NO}_3\text{+MT}}[NO_3]} \right). \qquad (3)$$
$$\text{MLH}^c \times \text{ws}^d$$

The rate constants and their temperature dependence were from Atkinson *et al.* (2004, 2006), and the fitting parameters *a, b, c,* and *d* can be found in Kontkanen *et al.* (2016). Figure S3 (found in Supplementary Information) illustrates the validation of the developed monoterpene proxy by the inter-comparisons with observational data. As shown in the Supplementary Information, $[\text{MT}]_{\text{proxy}}$ correlated well with the measured monoterpene concentration from 2010–2019, when MT measurements were available (see Fig. S3 in the Supplementary Information; r = 0.64).

Calculation of OH and NO_3 concentrations

The OH proxy concentration was estimated using the measured UVB data with the derived parameterization from Petäjä *et al.* (2009):

$$[\text{OH}]_{\text{proxy}} = \left(\frac{8.4 \times 10^{-7}}{8.6 \times 10^{-10}}\,\text{UVB}^{0.32} \right)^{1.92}. \qquad (4)$$

The NO_3 proxy concentration was determined analogous to Peräkylä *et al.* (2014), assuming a steady-state between the reaction of ozone and NO_2 via:

$$[\text{NO}_3] = k_{\text{O}_3\text{+NO}_2}[\text{O}_3][\text{NO}_2] \times \tau_{\text{NO}_3}. \qquad (5)$$

The NO_3 radical is an important oxidant during nighttime, when the lack of solar radiation increases its lifetime and concentration. An average NO_3 lifetime (τ_{NO3}) of 5 seconds was used to calculate daytime NO_3 concentrations (Peräkylä *et al*. 2014). For the estimation of nighttime NO_3 concentration, we used:

$$(\tau_{\text{NO}_3})^{-1} = k_{\text{NO}_3\text{+MT}}[\text{MT}] + k_{\text{NO}_3\text{+NO}}[\text{NO}] + \left(k_{N_2O_5\text{+H}_2\text{O}}[\text{H}_2\text{O}]\right) \times K[\text{NO}_2]. \qquad (6)$$

A constant MT value of 4.3×10^9 cm^{-3} (nighttime median from measurement; Kontkanen *et al.* 2016) was used to estimate the NO_3 nighttime lifetime for the period where no MT measurements were available (before 2010). The equilibrium constant K describing the reaction of NO_2 and NO to form N_2O_5 was $K = 5.1 \times 10^{-27}\exp(10871/T)$ analogues to Kontkanen *et al.* (2016).

HOM proxy

Here we derive a proxy for HOM concentration. Contrary to the H_2SO_4 and MT proxy derivations, the complete source, sink, and kinetic terms describing the formation and loss of HOM are difficult to derive. However, in this work we propose the following equation to describe the basic mechanisms:

$$\frac{d[\text{HOM}]}{dt} = k_a[\text{O}_3][\text{MT}] + k_b[\text{OH}][\text{MT}] - \text{CS}[\text{HOM}], \qquad (7)$$

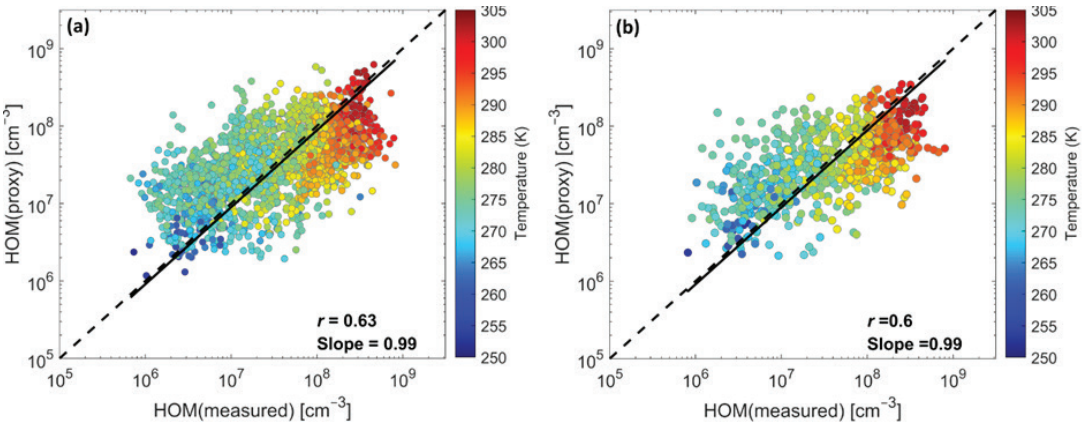

Fig. 1. Scatter plot of the HOM proxy concentration vs. measured HOM during 2016–2019 from (**a**) training dataset and (**b**) testing dataset. The scatter plots include data from all four seasons and considers both daytime and nighttime measurements. Data points are hourly averaged concentrations. The straight lines represent robust linear fits (intercept was set to zero), and the dashed lines are 1:1 line.

where k_a and k_b are temperature-dependent rate constants and corresponding yields of HOM that are eventually produced as consequences of the reactions of MT with O_3 and OH radical, respectively. Roldin *et al.* (2019) estimated that these three terms comprise the most important sources and sinks of HOM above the forest canopy. When moving towards ground level, dry deposition becomes increasingly important. However, to simplify the expression, we only consider the loss of HOM due to the CS. Although CS in our case was calculated using the diffusion coefficient of sulfuric acid, as the molecular size of all HOM cannot be inferred, this assumption is not expected to affect our derivation or calculation of the HOM proxy concentrations. Here, we exclude any nighttime and low radiation chemistry by the NO_3 radical as well as the contribution of other volatile organic compounds besides MT such as isoprene and sesquiterpenes. Due to this reason, we consider the oxidation of MT by O_3 and OH as the two major sources of HOM. The exclusion of nighttime oxidation of MT can be considered valid given that NPF in Hyytiälä takes place during light-hours (Dada *et al.* 2018), which are the focus of this study. Hence, the equation yields a HOM proxy concentration best used to describe daytime data when the contribution of the nighttime oxidation of MT is minimum (Hellén *et al.* 2018). Assuming a steady-state in the formation and loss of HOM, the HOM proxy concentration is:

$$[\mathrm{HOM}]\mathrm{proxy} = \frac{(k_a[\mathrm{O_3}] + k_b[\mathrm{OH}])[\mathrm{MT}]}{\mathrm{CS}}, \quad (8)$$

where parameters k_a and k_b were derived by fitting HOM concentrations measured in Hyytiälä. The data used for the HOM proxy development were from the observational data from SMEAR II station from 2016–2019. The dataset was divided into training dataset (75%) and testing dataset (25%), where the training dataset was used to train the model and to obtain the coefficients k_a and k_b using the optimization algorithm "*fmincon*" embedded in MATLAB (R2022b). Our data were resampled 1000 times using the bootstrap method, for also accounting for the accuracy of our k values as well as the predication error (Efron and Tibshirani, 1994). For the resampling we assumed both HOM concentrations and all related predictor variables to be affected by independent systematic errors between their lower and upper accuracy limits. More details on the bootstrap resampling method and uncertainty introduction can be found in Dada *et al.* (2020).

The obtained parameters k_a and k_b were $(1.8\pm0.063)\times10^{-26}\exp(-640/T)$ and $(3.25\pm7.1)\times10^{-16}\exp(440/T)$ cm^3 s^{-1}, respectively.

The training result of the HOM proxy is shown in Fig. 1a, and the proxy is further evaluated in this study and tested against an independent dataset, shown in Fig. 1b. Addition-

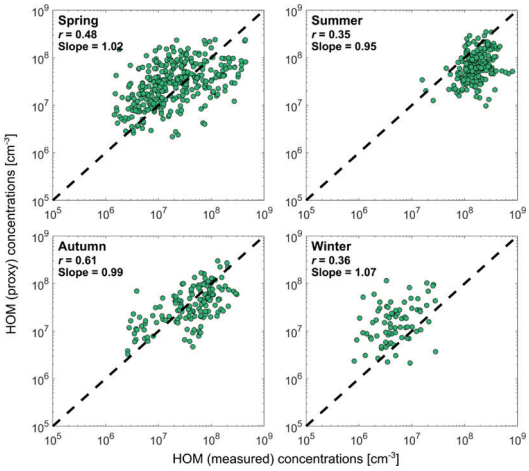

Fig. 2. Scatter plot of the HOM proxy concentration vs. measured HOM during 2016–2019 when HOM measurements were available. The subplots include data from four seasons separately and consider both daytime and nighttime measurements. Data points are hourly averaged concentrations from testing dataset. The Pearson correlation coefficients (r) and slopes (estimated from robust linear fit with intercept set to be zero) are displayed in each subplot. The dashed lines are 1:1 line.

ally, seasonal comparison between measured and proxy concentrations from the testing dataset is also displayed in Fig. 2. Although the newly developed HOM proxy method is only a relatively simple approximation of the source and sink terms describing the formation and loss of HOM, the estimated HOM proxy correlated well with the measured HOM concentration (r = 0.63 training dataset, r = 0.6 testing dataset; Fig. 1). Also, the cumulative distribution function (CDF) shows that the HOM proxy has a high prediction power of at least 70% as the cumulative error at accurate prediction (x = 0) is around 0.3 (see Fig. S4 in the Supplementary Information).

NPF event classification and particle formation rates

Daytime NPF events are classified following the method introduced by Dal Maso *et al.* (2005) and Kulmala *et al.* (2012). An event is recognized when a persistent new mode of particles (< 25 nm) appears in the DMPS particle number size distribution and exhibits growth toward the Aitken mode. NPF events are further subdivided into classes Ia, Ib and II. Class I NPF events are those during which a growth rate can be calculated. Class II events are those during which an event is observed in the DMPS particle size distribution, however a growth rate and thus an accurate formation rate cannot be retrieved due to fluctuations in concentrations and mode diameter. As we study the long-term trends on particle formation rates in this paper, we include only Class I events when tackling particle concentrations and formation rates in section "Trends of new particle formation rate and connection to precursors". This means that any possible contributions of smaller-scale NPF phenomena (e.g. nighttime clustering events; Rose *et al.* 2018) are excluded from this study.

Particle formation rates are calculated using the equation provided by Kulmala *et al.* (2012), Eq (9). The formation rates at 3 nm, J_3, are calculated considering the sources and sinks of particles within the size bin 3–25 nm. While the particles within the size bin are produced via NPF, they are lost to coagulation to preexisting particles or due to growth outside of the size bin. The growth rates (also those included in the J_3 calculation) were obtained by fitting lognormal functions to the measured particle number from the DMPS data (Hussein *et al.* 2005).

The start and end times of each NPF event can be determined from 2006 onwards based on the evolution of negatively charged particles in the size bin 2.5–4 nm observed in the NAIS using the automated method and threshold values proposed by Dada *et al.* (2018). Since NAIS data were not available before 2006, we chose the daytime between 9:00 and 16:00 (local time) as the NPF time windows in this study based on previous findings at the site (Dada *et al.* 2017) to make the data analysis consistent from 1996 to 2019.

Results and Discussion

Trends of ambient temperature, $[MT]_{proxy}$, $[HOM]_{proxy}$, SO_2 and $[H_2SO_4]_{proxy}$

Figure 3 shows the time series of ambient air temperature, $[MT]_{proxy}$, $[HOM]_{proxy}$, $[SO_2]$, and

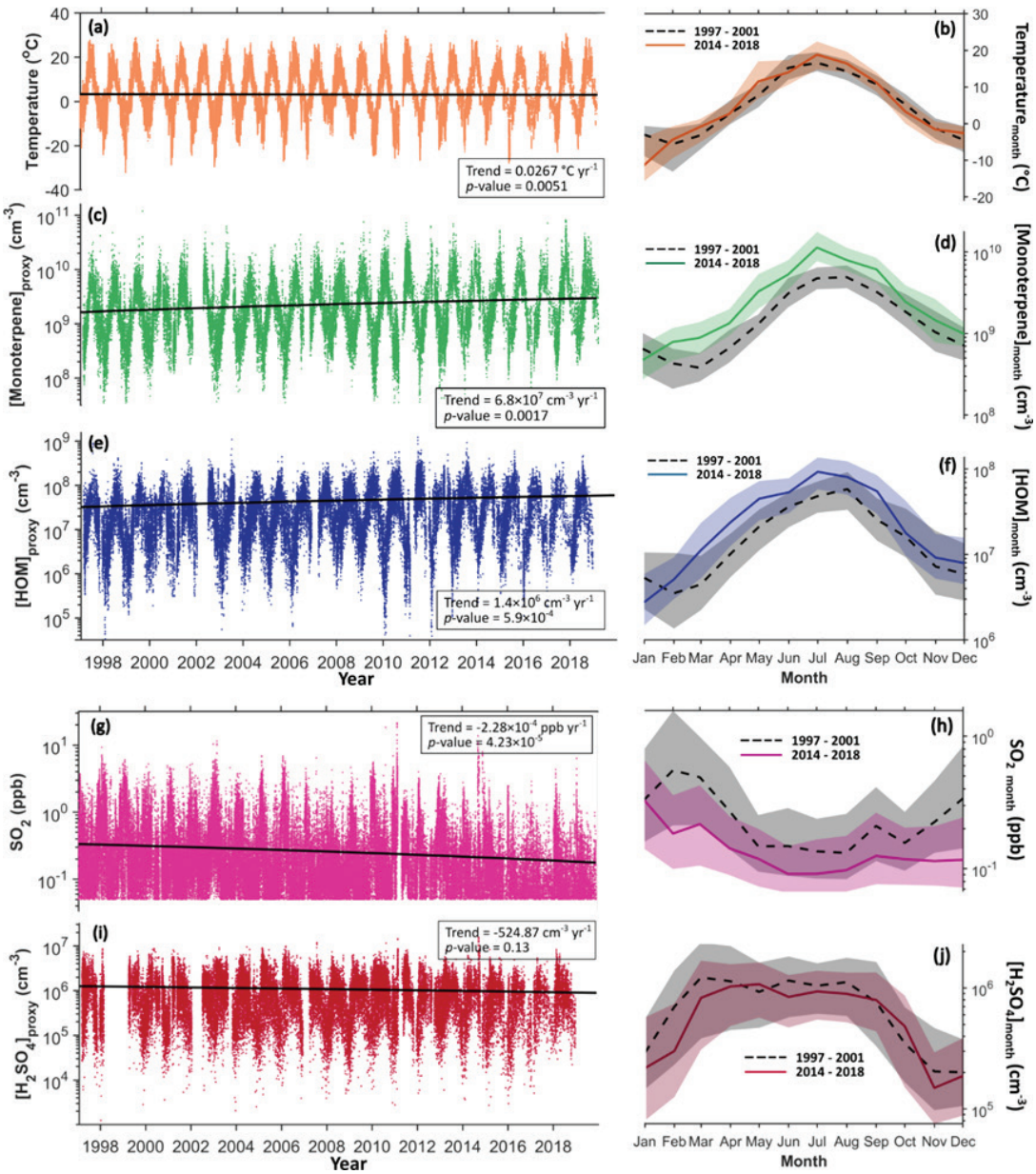

Fig. 3. Time series of (**a**) long-term ambient temperature; (**c**) $[MT]_{proxy}$; (**e**) $[HOM]_{proxy}$; (**g**) SO_2 mixing ratio; and (**i**) $[H_2SO_4]_{proxy}$ in Hyytiälä from 1997 to 2019 and their monthly medians during 1997 to 2001 and 2014 to 2018 (**b**, **d**, **f**, **h** and **j**). The data points were hourly ones. The solid black lines and trends showed linear fittings and slopes of fitted lines, respectively. The shaded areas denoted the values from the 25th to 75th percentile. For measured SO_2, the data points with SO_2 concentrations lower than the instrument detection limit (i.e., 0.05 ppb) of SO_2 monitor were removed.

$[H_2SO_4]_{proxy}$ in Hyytiälä during the last two decades. Associated with global warming, the ambient temperature over the boreal forest is increasing. Linear least squares fit to all observations from 1997 to 2019 yields a slope of +0.0267 ºC yr^{-1} (Fig. 3a), almost twice the rising rate of the global average temperature since 1970 (IPCC 2018). Previous studies have also shown that climate warming is more evident in higher latitudes than in low latitudes (Semenov 2012,

Xu *et al.* 2017). Based on the inter-comparison of monthly median values obtained from 1997 to 2001 and 2014 to 2018, the temperatures in June and July were slightly higher during 2014 to 2018 than that during 1997 to 2001 (Fig. 3b).

The emission rates of most biogenic VOCs show an exponential response to temperature variations (Guenther *et al.* 1993, Peñuelas and Llusia 2003). It has been also found that biogenic VOC emissions from the boreal forest in Hyytiälä are dominated by monoterpenes (Patokoski *et al.* 2014, Hellén *et al.* 2018). Therefore, a $[MT]_{proxy}$ was calculated for the last two decades to evaluate the long-term trends of VOC concentration in Hyytiälä (Kontkanen *et al.* 2016). The temperature-dependent seasonal variations of $[MT]_{proxy}$ have similar monthly variations that peak at summertime (Fig. 3c). The average trends suggest increasing monoterpene concentrations associated with the increasing temperatures, with a slope of 6.8×10^{7} molecules cm^{-3} yr^{-1}. Correspondingly, the concentration of $[HOM]_{proxy}$ increased gradually during the last two decades, with an annual increase rate of 1.6×10^{6} molecules cm^{-3} yr^{-1} (Fig. 3e). The seasonal fluctuations in HOM also peaked in summer when ambient temperature and monoterpene concentration reached the highest levels (Figs. 3b, d, f, and 2). In addition to these high records in summer, the abundance of MT and HOM estimated by the proxies during 2014 to 2018 are notably higher than that during 1997 to 2001.

In contrast to the increase in biogenic VOCs and HOM, SO_2 emissions in Europe show strong decreases since 1990 due to a combination of control measures, such as the promotion of low-sulfur fuels and the application of flue gas desulfurization techniques (EEA, 2023). Indeed, the SO_2 mixing ratio in Hyytiälä displayed a declining trend from 1996 to 2019 (Fig. 3g). The linear fitting suggests an annual decreasing rate of -4×10^{-3} ppb yr^{-1} for the SO_2 mixing ratio. Compared to the years 1997–2001, the SO_2 mixing ratio in 2014-2018 was significantly lower especially from November to April (Fig. 3h). Associated with the decreasing SO_2 mixing ratio, $[H_2SO_4]_{proxy}$ shows a slight decreasing trend of –524.87 molecules cm^{-3} yr^{-1} (Fig. 3i). The $[H_2SO_4]_{proxy}$ shows a rising concentrations in early spring, consistent with a decreasing level of SO_2 at that time (Fig. 3h and j) and with previous studies from the same site (Dada *et al.* 2017).

Trends of new particle formation rate and connection to precursors

During the years 1996–2019, a total of 1902 NPF days were observed (Fig. 4), with the highest frequency in springtime (Fig. 5a) as reported earlier at this site (Nieminen *et al.* 2014, Dada *et al.* 2017). The annual NPF frequency from 1996 to 2019 showed a decreasing trend, with an average reduction of –0.44 % yr^{-1} (Fig. 4a). From the intercomparison of monthly variations between 1997 to 2001 and 2014 to 2018, the decline in NPF frequency is the clearest during springtime, while the difference is less pronounced during the other NPF peak in autumn (Figs. 4a and S5b in the Supplementary Information). In winter, NPF events occurred at very low frequency in Hyytiälä, and during some months NPF was absent (Fig. 5a). Consistently, the nucleation mode (3–25 nm) particle number concentration ($N_{3\text{-}25}$) had a decreasing trend during all NPF event periods. The average annual reduction rate of $N_{3\text{-}25}$ was –6 cm^{-3} yr^{-1} (Fig. 4b). From 1996 to 2019, the monthly median J_3 for all NPF events decreased at an average trend of -9.3×10^{-3} cm^{-3} s^{-1} yr^{-1} (Fig. 4c). The monthly distribution of J_3 showed the highest values in spring, along with the highest concentrations of H_2SO_4 (Fig. 5a and b), consistent with previous long-term studies in Hyytiälä (Dada *et al.* 2017). As shown in Fig. 5, despite the highest HOM concentrations in summer, the J_3 values were higher in spring and autumn than in summer. This phenomenon may be attributed to higher CS and temperature in summer (Dada *et al.* 2017). On the other hand, the median $GR_{3\text{-}25}$ remained practically constant over the past decades with an insignificant negative slope of -6.3×10^{-3} nm h^{-1} yr^{-1} (Fig. 4d). Sulfuric acid is estimated to contribute only to a small fraction of nucleation mode growth in Hyytiälä (Kulmala *et al.* 1998, Kirkby *et al.* 2016, Bianchi *et al.* 2016). However, the higher temperature (especially in summer) which can alter the HOM

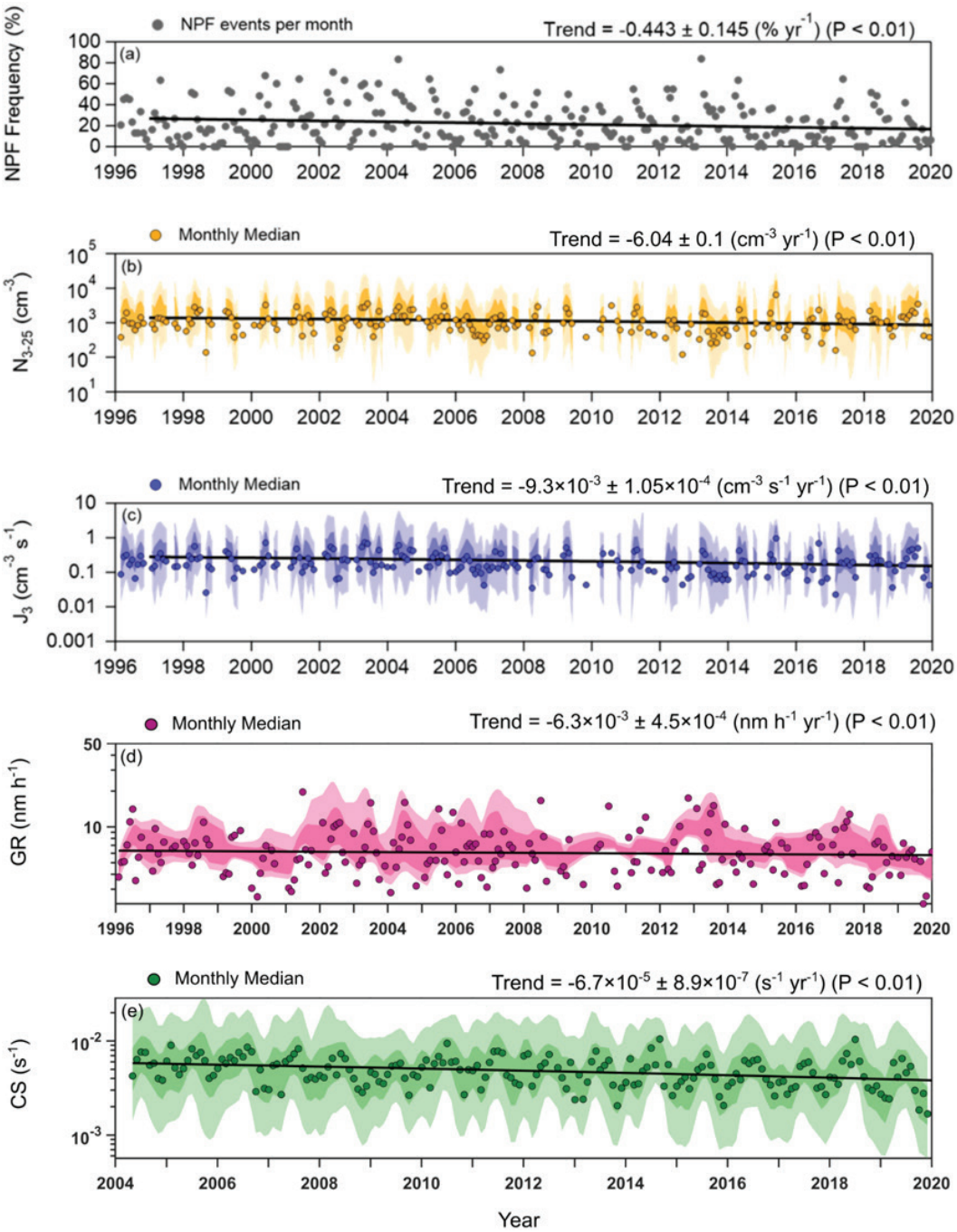

Fig. 4. Long-term variability of (**b**) NPF frequency particle number concentration ($N_{3\text{-}25}$); (**b**) particle formation rate J_3; (**c**) growth rates at 3–25 nm particles ($GR_{3\text{-}25}$); (**d**) condensation sink (CS); and (**e**) in Hyytiälä. The markers are fraction of NPF events per month in panel (**a**) and monthly median values in the rest. The dark shaded areas represent the 25th and 75th percentiles while the light shaded areas are the 5th and 95th percentiles. The solid lines show the linear fitting trends of different variables.

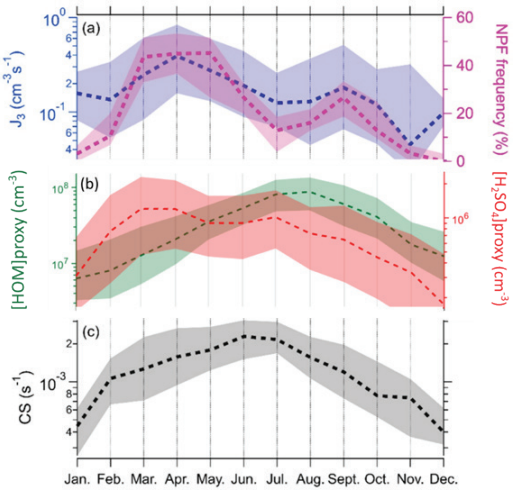

Fig. 5. Median monthly patterns of (**a**) J_3 and NPF frequency; (**b**) $[HOM]_{proxy}$ and $[H_2SO_4]_{proxy}$; and (**c**) CS for all NPF events during the entire observational period. For the CS data, before 2004, the daytime hourly data points from 09:00 to 16:00 of each event were selected. After 2004, the hourly data points were chosen based on the start and end times of each event which were obtained from NAIS data. The shaded areas showed the values from the 25th to 75th percentile.

volatility distribution may lead to less effective contribution of HOM to nucleation and initial growth (Simon *et al.* 2020).

At the same time, CS showed a decreasing trend of $–6.7\times10^{–5} \pm 8.9\times10^{–7}$ s$^{–1}$ yr$^{–1}$ between 1996 and 2019 (Fig. 4e). The decrease in CS, which is closely related to the total surface area of accumulation mode particles, can be attributed to a combination of several factors. First, the CS associated with the growth of newly formed particles has probably decreased as a result of the decreasing trend in the nucleation mode particle number concentration and no trend in their growth rate. Second, decreasing trends in total particle number concentrations have been observed in both Hyytiälä (Luoma *et al.* 2021) and Europe (Asmi *et al.* 2013), which suggests that also primary particle emissions affecting our site have decreased. Third, the overall accumulation of secondary particulate matter originating from anthropogenic precursors, especially from SO_2 and VOCs but possibly also from nitrogen oxides (NO_x) and ammonia (NH_3), into pre-existing particles has decreased during the past few decades.

Previous studies have confirmed that both H_2SO_4 and low volatility HOM can play essential roles in NPF (Sipilä *et al.* 2010, Ehn *et al.* 2014, Kirkby *et al.* 2016, Tröstl *et al.* 2016, Yan *et al.* 2020, Dada *et al.* 2023b). The contrasting long-term trends in H_2SO_4 and HOM raise the question of how they influence the occurrence and intensity of NPF events in the boreal forest environment of Hyytiälä, Finland. The decline of $[H_2SO_4]_{proxy}$ concentrations may lead to the particle formation driven less by the acid-base mechanism, whereas the increasing trend of $[HOM]_{proxy}$ concentrations might elevate the probability of organic vapors contributing to particle formation. Such observations may imply a potential shift on the NPF mechanism more towards the organic-driven particle formation pathways. Moreover, the ion-induced nucleation (IIN) has been found to be the dominant pathway in particle formation during the initial growth up to 3 nm when H_2SO_4 concentrations are low in the atmosphere (Eichkorn *et al.* 2002, Lee *et al.* 2003). From CLOUD chamber experiments, Lehtipalo *et al.* (2018) discovered that the IIN is about an order of magnitude stronger than in the presence of H_2SO_4–NH_3. This is supported by the study of Yan *et al.* (2018) who found increasing amounts of biogenic ion-clusters as a function of an increased HOM to H_2SO_4 ratio. In parallel, Rose e*t al.* (2018) reported nocturnal ion-induced biogenic driven clustering events occurring at nights, when H_2SO_4 concentrations were too low to trigger a ternary H_2SO_4–NH_3 nucleation (median H_2SO_4 concentration 8.4×10^5 cm$^{–3}$). With the observed H_2SO_4 concentrations decrease of –524.87 cm$^{–3}$ y$^{–1}$, together with the increasing trend in HOM concentrations 1.6×10^6 cm$^{–3}$ y$^{–1}$, the particle formation mechanism can be speculated to shift towards a weaker ion-induced biogenic driven mechanism, which might only partly compensate for the decrease in particle formation rates. Associated with the almost constant growth rate, such conclusion could lead to more quiet new particle formation events (Kulmala *et al.* 2022b).

Although fewer particles are formed, indicated by a decreasing J_3 (Fig. 4c), they still grow at the average speed (steady $GR_{3\text{-}25}$) regardless of the increase in HOM concentrations and decrease in CS. Such an observation could imply

an overall decrease in CCN concentrations but could only be confirmed via inspecting long-term measurements of CCN in a regional context.

Summary and Conclusion

In this study, the trends of ambient temperature, new particle formation frequencies, SO_2, $[MT]_{proxy}$, $[H_2SO_4]_{proxy}$, CS and $[HOM]_{proxy}$ have been reported on the basis of over 20 years of observations collected at a boreal forest station. To obtain the HOM trend, a new HOM proxy was derived. In response to global warming and pollution controls, the increasing trend of temperature, monoterpenes and HOM, the declining trends of anthropogenic SO_2, H_2SO_4, and primary particle emissions were observed. In addition, during the past 20 years, the intensity (i.e., J_3) and frequency of NPF events have both been declining which might imply that H_2SO_4 is still more important compared to HOM as the precursor vapor in the initial steps of NPF. At this rate of persistent increase of HOM and decrease of H_2SO_4, a change in particle formation pathway from sulfuric acid dominated to HOM dominated is expected in the future.

Due to the continued temperature increase, especially in summer, concurrent with global warming, a significant increase in VOC emissions from vegetation is observed and expected to further continue. However, environmental stress could also cause changes in the structure of plant leaves and therefore the emitted VOC types (Daussy and Staudt 2020, Zhao *et al.* 2017). Such changes could alter the volatility distribution of HOM leading to changes in the contribution of HOM in the early stage of NPF (Dada *et al.* 2023a). For that purpose, the synergy between the increasing temperature and the changing HOM amount, composition, and volatility on NPF needs further detailed investigations. Our results provide insights into long-term trends of monoterpenes, H_2SO_4, and HOM, and their potential roles in NPF in the boreal forest environment. Given the significant role of NPF events in forming CCN, our findings on a decrease in NPF frequency and intensity at an almost constant growth rate help further improve our understating of the contribution of NPF to atmosphere-cloud interactions in the boreal forest in a future affected by climate change.

Acknowledgements: We acknowledge the following projects: ACCC Flagship funded by the Academy of Finland grant number 337549, "Quantifying carbon sink, CarbonSink+ and their interaction with air quality" INAR project funded by Jane and Aatos Erkko Foundation, European Research Council (ERC) project ATM-GTP (No. 742206), BAE (No. 101076311) and CHAPAs (grant no. 850614), Academy of Finland projects 310682, 325656, 311932, 334792, 316114, 325647, 325681, 333397, 328616, 357902, 345510, 347782 and 337550 (the UEF part of the Flagship funding) and 346371 (Centre of Excellence). M.K. acknowledges support from the Academy of Finland via his academy professorship (302958). The work was partially supporte by European Union via Non-CO2 Forcers and their Climate, Weather, Air Quality and Health Impacts (FOCI), and CRiceS (No 101003826), EMME-CARE (856612) and FORCeS (821205). University of Helsinki support via ACTRIS-HY is acknowledged. Support of the technical and scientific staff in Hyytiälä is gratefully acknowledged. This work received funding from the Swiss National Science Foundation Ambizione grants PZPGP2_201992 and PZ00P2_216181. This research has received funding from the Vienna Science and Technology Fund (WWTF) through project VRG22-003.

Supplementary Information: The supplementary information related to this article is available online at: http://www.borenv.net/BER/archive/pdfs/ber29/ber29-035-052-supplement.pdf

Author Contributions: This study was initiated as part of intensive course in Hyytiälä in March 2020. X.L., H.L., L.Y., R.W.J., L.V., L.D., R.B., and H.U. analyzed the data. X.L., H.L. and L.Y. made the final figures. H.L., L.Y., M.K., F.B., L.D., D.S., T.N., X.L., J.K., K.L., T.P., and V.M.K. interpreted the results. X.L., H.L., L.Y. and L.D. wrote the manuscript with contributions from all co-authors.

Declaration of competing interest: The authors declare that they have no known competing financial interests.

References

Aalto P., Hämeri K., Becker E., Weber R., Salm J., Mäkelä J.M., Hoell C., O'dowd C.D., Hansson H.-C., Väkevä M., Koponen I.K., Buzorius G. & Kulmala M. 2001. Physical characterization of aerosol particles during nucleation events. *Tellus B: Chemical and Physical Meteorology* 53: 344–358.

Almeida J., Schobesberger S., Kürten A., Ortega I.K., Kupiainen-Määttä O., Praplan A.P., Adamov A., Amorim A., Bianchi F., Breitenlechner M., David A., Dommen J., Donahue N.M., Downard A., Dunne E., Duplissy J., Ehrhart S., Flagan R.C., Franchin A., Guida R., Hakala J., Hansel A., Heinritzi M., Henschel H., Jokinen T., Junninen H., Kajos M., Kangasluoma J., Keskinen H., Kupc A., Kurtén T., Kvashin A.N., Laaksonen A., Lehtipalo K., Leiminger M., Leppä J., Loukonen V., Makhmutov V., Mathot S., McGrath M.J., Nieminen T., Olenius T., Onnela A., Petäjä T., Riccobono F., Riipinen I., Rissanen M., Rondo L., Ruuskanen T., Santos F.D., Sarnela N., Schallhart S., Schnitzhofer R., Seinfeld J.H., Simon M., Sipilä M., Stozhkov Y., Stratmann F., Tomé A., Tröstl J., Tsagkogeorgas G., Vaattovaara P., Viisanen Y., Virtanen A., Vrtala A., Wagner P.E., Weingartner E., Wex H., Williamson C., Wimmer D., Ye P., Yli-Juuti T., Carslaw K.S., Kulmala M., Curtius J., Baltensperger U., Worsnop D.R., Vehkamäki H. & Kirkby J. 2013. Molecular understanding of sulphuric acid–amine particle nucleation in the atmosphere. *Nature* 502: 359–363.

Asmi A., Collaud Coen M., Ogren J.A., Andrews E., Sheridan P., Jefferson A., Weingartner E., Baltensperger U., Bukowiecki N., Lihavainen H., Kivekäs N., Asmi E., Aalto P.P., Kulmala M., Wiedensohler A., Birmili W., Hamed A., O'Dowd C., G Jennings S., Weller R., Flentje H., Fjaeraa A.M., Fiebig M., Myhre C.L., Hallar A.G., Swietlicki E., Kristensson A. & Laj P. 2013. Aerosol decadal trends – Part 2: In-situ aerosol particle number concentrations at GAW and ACTRIS stations. Atmospheric Chemistry and Physics 13: 895–916.

Atkinson R., Baulch D.L., Cox R.A., Crowley J.N., Hampson R.F., Hynes R.G., Jenkin M.E., Rossi M.J. & Troe J. 2004. Evaluated kinetic and photochemical data for atmospheric chemistry: Volume I - gas phase reactions of O_x, HO_x, NO_x and SO_x species. *Atmospheric Chemistry and Physics* 4: 1461–1738.

Atkinson R., Baulch D.L., Cox R.A., Crowley J.N., Hampson R.F., Hynes R.G., Jenkin M.E., Rossi M.J., Troe J. & IUPAC Subcommittee. 2006. Evaluated kinetic and photochemical data for atmospheric chemistry: Volume II – gas phase reactions of organic species. *Atmospheric Chemistry and Physics* 6: 3625–4055.

Bianchi F., Tröstl J., Junninen H., Frege C., Henne S., Hoyle C.R., Molteni U., Herrmann E., Adamov A., Bukowiecki N., Chen X., Duplissy J., Gysel M., Hutterli M., Kangasluoma J., Kontkanen J., Kürten A., Manninen H.E., Münch S., Peräkylä O., Petäjä T., Rondo L., Williamson C., Weingartner E., Curtius J., Worsnop D.R., Kulmala M., Dommen J. & Baltensperger U. 2016. New particle formation in the free troposphere: A question of chemistry and timing. Science (New York, N.Y.) 352: 1109–1112.

Bianchi F., Kurtén T., Riva M., Mohr C., Rissanen M.P., Roldin P., Berndt T., Crounse J.D., Wennberg P.O., Mentel T.F., Wildt J., Junninen H., Jokinen T., Kulmala M., Worsnop D.R., Thornton J.A., Donahue N., Kjaergaard H.G. & Ehn M. 2019. Highly Oxygenated Organic Molecules (HOM) from Gas-Phase Autoxidation Involving Peroxy Radicals: A Key Contributor to Atmospheric Aerosol. *Chemical Reviews* 119: 3472–3509.

Bussotti F. & Pollastrini M. 2021. Revisiting the concept of stress in forest trees at the time of global change and issues for stress monitoring. *Plant Stress* 2: 100013.

Charlson R.J., Schwartz S.E., Hales J.M., Cess R.D., Coakley J.A., Hansen J.E. & Hofmann D.J. 1992. Climate Forcing by Anthropogenic Aerosols. *Science* 255: 423–430.

Chu B., Kerminen V.-M., Bianchi F., Yan C., Petäjä T. & Kulmala M. 2019. Atmospheric new particle formation in China. *Atmospheric Chemistry and Physics* 19: 115–138.

Clarke A.D., Freitag S., Simpson R.M.C., Hudson J.G., Howell S.G., Brekhovskikh V.L., Campos T., Kapustin V.N. & Zhou J. 2013. Free troposphere as a major source of CCN for the equatorial pacific boundary layer: long-range transport and teleconnections. *Atmospheric Chemistry and Physics* 13: 7511–7529.

Coffman D.J. & Hegg Dean.A. 1995. A preliminary study of the effect of ammonia on particle nucleation in the marine boundary layer. *Journal of Geophysical Research: Atmospheres* 100: 7147–7160.

Dada L., Paasonen P., Nieminen T., Buenrostro Mazon S., Kontkanen J., Peräkylä O., Lehtipalo K., Hussein T., Petäjä T., Kerminen V.-M., Bäck J. & Kulmala M. 2017. Long-term analysis of clear-sky new particle formation events and nonevents in Hyytiälä. *Atmospheric Chemistry and Physics* 17: 6227–6241.

Dada L., Chellapermal R., Buenrostro Mazon S., Paasonen P., Lampilahti J., Manninen H.E., Junninen H., Petäjä T., Kerminen V.-M. & Kulmala M. 2018. Refined classification and characterization of atmospheric new-particle formation events using air ions. *Atmospheric Chemistry and Physics* 18: 17883–17893.

Dada L., Ylivinkka I., Baalbaki R., Li C., Guo Y., Yan C., Yao L., Sarnela N., Jokinen T., Daellenbach K.R., Yin R., Deng C., Chu B., Nieminen T., Wang Y., Lin Z., Thakur R.C., Kontkanen J., Stolzenburg D., Sipilä M., Hussein T., Paasonen P., Bianchi F., Salma I., Weidinger T., Pikridas M., Sciare J., Jiang J., Liu Y., Petäjä T., Kerminen V.-M. & Kulmala M. 2020. Sources and sinks driving sulfuric acid concentrations in contrasting environments: implications on proxy calculations. *Atmospheric Chemistry and Physics* 20: 11747–11766.

Dada L., Stolzenburg D., Simon M., Fischer L., Heinritzi M., Wang M., Xiao M., Vogel A.L., Ahonen L., Amorim A., Baalbaki R., Baccarini A., Baltensperger U., Bianchi F., Daellenbach K.R., DeVivo J., Dias A., Dommen J., Duplissy J., Finkenzeller H., Hansel A., He X.-C., Hofbauer V., Hoyle C.R., Kangasluoma J., Kim C., Kürten A., Kvashnin A., Mauldin R., Makhmutov V., Marten R., Mentler B., Nie W., Petäjä T., Quéléver L.L.J., Saathoff H., Tauber C., Tome A., Molteni U., Volkamer R., Wagner R., Wagner A.C., Wimmer D., Winkler P.M., Yan C., Zha Q., Rissanen M., Gordon H., Curtius J., Worsnop D.R., Lehtipalo K., Donahue N.M., Kirkby J., El Haddad I. & Kulmala M. 2023a. Role of sesquiterpenes in biogenic new particle formation. Science Advances 9: eadi5297.

Dada L., Okuljar M., Shen J., Olin M., Wu Y., Heimsch L., Herlin I., Kankaanrinta S., Lampimäki M., Kalliokoski J., Baalbaki R., Lohila A., Petäjä T., Dal Maso M., Duplissy J., Kerminen V.-M. & Kulmala M. 2023b. The synergistic role of sulfuric acid, ammonia and organics in particle formation over an agricultural land. *Environmental Science: Atmospheres* 3: 1195–1211.

Dal Maso M., Kulmala M., Riipinen I., Wagner R., Hussein T., Aalto P.P. & Lehtinen K.E.J. 2005. Formation and growth of fresh atmospheric aerosols: eight years of aerosol size distribution data from SMEAR II, Hyytiälä, Finland. *Boreal Environment Research* 10: 323–336.

Daussy J. & Staudt M. 2020. Do future climate conditions change volatile organic compound emissions from Artemisia annua? Elevated CO2 and temperature modulate actual VOC emission rate but not its emission capacity. *Atmospheric Environment: X* 7: 100082.

Dunne E.M., Gordon H., Kürten A., Almeida J., Duplissy J., Williamson C., Ortega I.K., Pringle K.J., Adamov A., Baltensperger U., Barmet P., Benduhn F., Bianchi F., Breitenlechner M., Clarke A., Curtius J., Dommen J., Donahue N.M., Ehrhart S., Flagan R.C., Franchin A., Guida R., Hakala J., Hansel A., Heinritzi M., Jokinen T., Kangasluoma J., Kirkby J., Kulmala M., Kupc A., Lawler M.J., Lehtipalo K., Makhmutov V., Mann G., Mathot S., Merikanto J., Miettinen P., Nenes A., Onnela A., Rap A., Reddington C.L.S., Riccobono F., Richards N.A.D., Rissanen M.P., Rondo L., Sarnela N., Schobesberger S., Sengupta K., Simon M., Sipilä M., Smith J.N., Stozkhov Y., Tomé A., Tröstl J., Wagner P.E., Wimmer D., Winkler P.M., Worsnop D.R. & Carslaw K.S. 2016. Global atmospheric particle formation from CERN CLOUD measurements. *Science* 354: 1119–1124.

EEA, 2019. European Uniion Emission Inventory Report 1990–2017 under the UNECE Convention on Long-Range Transboundary Air Pollution (LRTAP). European Environment Agency, Copenhagen, Denmark.

EEA, European Union emission inventory report 1990-2018 — European Environment Agency: https://www.eea.europa.eu/publications/european-union-emission-inventory-report-1990-2018, last access: 22 August 2023.

Eerdekens G., Yassaa N., Sinha V., Aalto P.P., Aufmhoff H., Arnold F., Fiedler V., Kulmala M. & Williams J. 2009. VOC measurements within a boreal forest during spring 2005: on the occurrence of elevated monoterpene concentrations during night time intense particle concentration events. *Atmospheric Chemistry and Physics* 9: 8331–8350.

Efron B. & Tibshirani R. 1986. Bootstrap Methods for Standard Errors, Confidence Intervals, and Other Measures of Statistical Accuracy. *Statistical Science* 1: 54–75.

Ehn M., Thornton J.A., Kleist E., Sipilä M., Junninen H., Pullinen I., Springer M., Rubach F., Tillmann R., Lee B., Lopez-Hilfiker F., Andres S., Acir I.-H., Rissanen M., Jokinen T., Schobesberger S., Kangasluoma J., Kontkanen J., Nieminen T., Kurtén T., Nielsen L.B., Jørgensen S., Kjaergaard H.G., Canagaratna M., Maso M.D., Berndt T., Petäjä T., Wahner A., Kerminen V.-M., Kulmala M., Worsnop D.R., Wildt J. & Mentel T.F. 2014. A large source of low-volatility secondary organic aerosol. *Nature* 506: 476–479.

Eichkorn S., Wilhelm S., Aufmhoff H., Wohlfrom K.H. & Arnold F. 2002. Cosmic ray-induced aerosol-formation: First observational evidence from aircraft-based ion mass spectrometer measurements in the upper troposphere. Geophysical Research Letters 29: 43-1-43–44.

Gordon H., Kirkby J., Baltensperger U., Bianchi F., Breitenlechner M., Curtius J., Dias A., Dommen J., Donahue N.M., Dunne E.M., Duplissy J., Ehrhart S., Flagan R.C., Frege C., Fuchs C., Hansel A., Hoyle C.R., Kulmala M., Kürten A., Lehtipalo K., Makhmutov V., Molteni U., Rissanen M.P., Stozkhov Y., Tröstl J., Tsagkogeorgas G., Wagner R., Williamson C., Wimmer D., Winkler P.M., Yan C. & Carslaw K.S. 2017. Causes and importance of new particle formation in the present-day and preindustrial atmospheres. *Journal of Geophysical Research: Atmospheres* 122: 8739–8760.

Guenther A.B., Zimmerman P.R., Harley P.C., Monson R.K. & Fall R. 1993. Isoprene and monoterpene emission rate variability: Model evaluations and sensitivity analyses. *Journal of Geophysical Research: Atmospheres* 98: 12609–12617.

Hakola H., Hellén H., Hemmilä M., Rinne J. & Kulmala M. 2012. In situ measurements of volatile organic compounds in a boreal forest. *Atmospheric Chemistry and Physics* 12: 11665–11678.

Hari P. & Kulmala M. 2005. Station for Measuring Ecosystem-Atmosphere Relations (SMEAR II). *Boreal Environment Research* 10: 315–322.

Hellén H., Praplan A.P., Tykkä T., Ylivinkka I., Vakkari V., Bäck J., Petäjä T., Kulmala M. & Hakola H. 2018. Long-term measurements of volatile organic compounds highlight the importance of sesquiterpenes for the atmospheric chemistry of a boreal forest. *Atmospheric Chemistry and Physics* 18: 13839–13863.

Holopainen J.K. 2011. Can forest trees compensate for stress-generated growth losses by induced production of volatile compounds? *Tree Physiology* 31: 1356–1377.

Holopainen J.K., Virjamo V., Ghimire R.P., Blande J.D., Julkunen-Tiitto R. & Kivimäenpää M. 2018. Climate Change Effects on Secondary Compounds of Forest Trees in the Northern Hemisphere. *Frontiers in Plant Science* 9.

Hussein T., Dal Maso M., Petäjä T., Koponen I.K., Paatero P., Aalto P.P., Hämeri K. & Kulmala M. 2005. Evaluation of an automatic algorithm for fitting the particle number size distributions. *Boreal Environment Research* 10: 337–355.

IPCC, 2018: Global warming of 1.5°C. An IPCC Special Report on the impacts of global warming of 1.5°C above pre-industrial levels and related global greenhouse gas emission pathways, in the context of strengthening the global response to the threat of climate change, sustainable development, and efforts to eradicate poverty [V. Masson-Delmotte, P. Zhai, H. O. Pörtner, D. Roberts, J. Skea, P.R. Shukla, A. Pirani, W. Moufouma-Okia, C. Péan, R. Pidcock, S. Connors, J. B. R. Matthews, Y. Chen, X. Zhou, M. I. Gomis, E. Lonnoy, T. Maycock, M. Tignor, T. Waterfield (eds.)]. In Press.

Jokinen T., Sipilä M., Junninen H., Ehn M., Lönn G., Hakala J., Petäjä T., Mauldin R.L.I., Kulmala M. & Worsnop D.R. 2012. Atmospheric sulphuric acid and neutral cluster measurements using CI-APi-TOF. *Atmospheric Chemistry and Physics* 12: 4117–4125.

Junninen H., Ahonen L., Bianchi F., Quéléver L., Schallhart S., Dada L., Manninen H.E., Leino K., Lampilahti J., Buenrostro Mazon S., Rantala P., Räty M., Kontkanen J., Negri S., Aliaga D., Garmash O., Alekseychik P., Lipp H., Tamme K., Levula J., Sipilä M., Ehn M., Worsnop D., Zilitinkevich S., Mammarella I., Rinne J., Vesala T., Petäjä T., Kerminen V.-M. & Kulmala M. 2022. Terpene emissions from boreal wetlands can initiate stronger atmospheric new particle formation than boreal forests. Communications Earth & Environment 3: 1–9.

Kerminen V.-M., Chen X., Vakkari V., Petäjä T., Kulmala M. & Bianchi F. 2018. Atmospheric new particle formation and growth: review of field observations. *Environmental Research Letters* 13: 103003.

Kirkby J., Curtius J., Almeida J., Dunne E., Duplissy J., Ehrhart S., Franchin A., Gagné S., Ickes L., Kürten A., Kupc A., Metzger A., Riccobono F., Rondo L., Schobesberger S., Tsagkogeorgas G., Wimmer D., Amorim A., Bianchi F., Breitenlechner M., David A., Dommen J., Downard A., Ehn M., Flagan R.C., Haider S., Hansel A., Hauser D., Jud W., Junninen H., Kreissl F., Kvashin A., Laaksonen A., Lehtipalo K., Lima J., Lovejoy E.R., Makhmutov V., Mathot S., Mikkilä J., Minginette P., Mogo S., Nieminen T., Onnela A., Pereira P., Petäjä T., Schnitzhofer R., Seinfeld J.H., Sipilä M., Stozhkov Y., Stratmann F., Tomé A., Vanhanen J., Viisanen Y., Vrtala A., Wagner P.E., Walther H., Weingartner E., Wex H., Winkler P.M., Carslaw K.S., Worsnop D.R., Baltensperger U. & Kulmala M. 2011. Role of sulphuric acid, ammonia and galactic cosmic rays in atmospheric aerosol nucleation. *Nature* 476: 429–433.

Kirkby J., Duplissy J., Sengupta K., Frege C., Gordon H., Williamson C., Heinritzi M., Simon M., Yan C., Almeida J., Tröstl J., Nieminen T., Ortega I.K., Wagner R., Adamov A., Amorim A., Bernhammer A.-K., Bianchi F., Breitenlechner M., Brilke S., Chen X., Craven J., Dias A., Ehrhart S., Flagan R.C., Franchin A., Fuchs C., Guida R., Hakala J., Hoyle C.R., Jokinen T., Junninen H., Kangasluoma J., Kim J., Krapf M., Kürten A., Laaksonen A., Lehtipalo K., Makhmutov V., Mathot S., Molteni U., Onnela A., Peräkylä O., Piel F., Petäjä T., Praplan A.P., Pringle K., Rap A., Richards N.A.D., Riipinen I., Rissanen M.P., Rondo L., Sarnela N., Schobesberger S., Scott C.E., Seinfeld J.H., Sipilä M., Steiner G., Stozhkov Y., Stratmann F., Tomé A., Virtanen A., Vogel A.L., Wagner A.C., Wagner P.E., Weingartner E., Wimmer D., Winkler P.M., Ye P., Zhang X., Hansel A., Dommen J., Donahue N.M., Worsnop D.R., Baltensperger U., Kulmala M., Carslaw K.S. & Curtius J. 2016. Ion-induced nucleation of pure biogenic particles. *Nature* 533: 521–526.

Kolari P., Bäck J., Taipale R., Ruuskanen T.M., Kajos M.K., Rinne J., Kulmala M. & Hari P. 2012. Evaluation of accuracy in measurements of VOC emissions with dynamic chamber system. *Atmospheric Environment* 62: 344–351.

Kontkanen J., Paasonen P., Aalto J., Bäck J., Rantala P., Petäjä T. & Kulmala M. 2016. Simple proxies for estimating the concentrations of monoterpenes and their oxidation products at a boreal forest site. *Atmospheric Chemistry and Physics* 16: 13291–13307.

Kulmala M., Toivonen A., Mäkelä J.M. & Laaksonen A. 1998. Analysis of the growth of nucleation mode particles observed in Boreal forest. *Tellus B: Chemical and Physical Meteorology* 50: 449–462.

Kulmala M. 2003. How Particles Nucleate and Grow. *Science* 302: 1000–1001.

Kulmala M., Laakso L., Lehtinen K.E.J., Riipinen I., Dal Maso M., Anttila T., Kerminen V.-M., Hõrrak U., Vana M. & Tammet H. 2004a. Initial steps of aerosol growth. *Atmospheric Chemistry and Physics* 4: 2553–2560.

Kulmala M., Vehkamäki H., Petäjä T., Dal Maso M., Lauri A., Kerminen V.-M., Birmili W. & McMurry P.H. 2004b. Formation and growth rates of ultrafine atmospheric particles: a review of observations. *Journal of Aerosol Science* 35: 143–176.

Kulmala M., Kerminen V.-M., Anttila T., Laaksonen A. & O'Dowd C.D. 2004c. Organic aerosol formation via sulphate cluster activation. *Journal of Geophysical Research: Atmospheres* 109.

Kulmala M., Riipinen I., Sipilä M., Manninen H.E., Petäjä T., Junninen H., Maso M.D., Mordas G., Mirme A., Vana M., Hirsikko A., Laakso L., Harrison R.M., Hanson I., Leung C., Lehtinen K.E.J. & Kerminen V.-M. 2007. Toward Direct Measurement of Atmospheric Nucleation. *Science* 318: 89–92.

Kulmala M., Petäjä T., Nieminen T., Sipilä M., Manninen H.E., Lehtipalo K., Dal Maso M., Aalto P.P., Junninen H., Paasonen P., Riipinen I., Lehtinen K.E.J., Laaksonen A. & Kerminen V.-M. 2012. Measurement of the nucleation of atmospheric aerosol particles. *Nature Protocols* 7: 1651–1667.

Kulmala M., Kontkanen J., Junninen H., Lehtipalo K., Manninen H.E., Nieminen T., Petäjä T., Sipilä M., Schobesberger S., Rantala P., Franchin A., Jokinen T., Järvinen E., Äijälä M., Kangasluoma J., Hakala J., Aalto P.P., Paasonen P., Mikkilä J., Vanhanen J., Aalto J., Hakola H., Makkonen U., Ruuskanen T., Mauldin R.L., Duplissy J., Vehkamäki H., Bäck J., Kortelainen A., Riipinen I., Kurtén T., Johnston M.V., Smith J.N., Ehn M., Mentel T.F., Lehtinen K.E.J., Laaksonen A., Kerminen V.-M. & Worsnop D.R. 2013. Direct Observations of Atmospheric Aerosol Nucleation. *Science* 339: 943–946.

Kulmala M., Stolzenburg D., Dada L., Cai R., Kontkanen J., Yan C., Kangasluoma J., Ahonen L.R., Gonzalez-Carracedo L., Sulo J., Tuovinen S., Deng C., Li Y., Lehtipalo K., Lehtinen K.E.J., Petäjä T., Winkler P.M., Jiang J. & Kerminen V.-M. 2022a. Towards a concentration closure of sub-6 nm aerosol particles and sub-3 nm atmospheric clusters. Journal of Aerosol Science 159: 105878.

Kulmala M., Junninen H., Dada L., Salma I., Weidinger T., Thén W., Vörösmarty M., Komsaare K., Stolzenburg

D., Cai R., Yan C., Li X., Deng C., Jiang J., Petäjä T., Nieminen T. & Kerminen V.-M. 2022b. Quiet New Particle Formation in the Atmosphere. Frontiers in Environmental Science 10.

Kürten A., Rondo L., Ehrhart S. & Curtius J. 2012. Calibration of a Chemical Ionization Mass Spectrometer for the Measurement of Gaseous Sulfuric Acid. *The Journal of Physical Chemistry A* 116: 6375–6386.

Lappalainen H.K., Sevanto S., Bäck J., Ruuskanen T.M., Kolari P., Taipale R., Rinne J., Kulmala M. & Hari P. 2009. Day-time concentrations of biogenic volatile organic compounds in a boreal forest canopy and their relation to environmental and biological factors. *Atmospheric Chemistry and Physics* 9: 5447–5459.

Lathière J., Hauglustaine D.A., De Noblet-Ducoudré N., Krinner G. & Folberth G.A. 2005. Past and future changes in biogenic volatile organic compound emissions simulated with a global dynamic vegetation model. *Geophysical Research Letters* 32.

Lee S.-H., Reeves J.M., Wilson J.C., Hunton D.E., Viggiano A.A., Miller T.M., Ballenthin J.O. & Lait L.R. 2003. Particle Formation by Ion Nucleation in the Upper Troposphere and Lower Stratosphere. Science 301: 1886–1889.

Lehtipalo K., Yan C., Dada L., Bianchi F., Xiao M., Wagner R., Stolzenburg D., Ahonen L.R., Amorim A., Baccarini A., Bauer P.S., Baumgartner B., Bergen A., Bernhammer A.-K., Breitenlechner M., Brilke S., Buchholz A., Mazon S.B., Chen D., Chen X., Dias A., Dommen J., Draper D.C., Duplissy J., Ehn M., Finkenzeller H., Fischer L., Frege C., Fuchs C., Garmash O., Gordon H., Hakala J., He X., Heikkinen L., Heinritzi M., Helm J.C., Hofbauer V., Hoyle C.R., Jokinen T., Kangasluoma J., Kerminen V.-M., Kim C., Kirkby J., Kontkanen J., Kürten A., Lawler M.J., Mai H., Mathot S., Mauldin R.L., Molteni U., Nichman L., Nie W., Nieminen T., Ojdanic A., Onnela A., Passananti M., Petäjä T., Piel F., Pospisilova V., Quéléver L.L.J., Rissanen M.P., Rose C., Sarnela N., Schallhart S., Schuchmann S., Sengupta K., Simon M., Sipilä M., Tauber C., Tomé A., Tröstl J., Väisänen O., Vogel A.L., Volkamer R., Wagner A.C., Wang M., Weitz L., Wimmer D., Ye P., Ylisirniö A., Zha Q., Carslaw K.S., Curtius J., Donahue N.M., Flagan R.C., Hansel A., Riipinen I., Virtanen A., Winkler P.M., Baltensperger U., Kulmala M. & Worsnop D.R. 2018. Multicomponent new particle formation from sulfuric acid, ammonia, and biogenic vapors. *Science Advances* 4: eaau5363.

Lindfors V., Laurila T., Hakola H., Steinbrecher R. & Rinne J. 2000. Modeling speciated terpenoid emissions from the European boreal forest. *Atmospheric Environment* 34: 4983–4996.

Liu S., Xing J., Zhang H., Ding D., Zhang F., Zhao B., Sahu S.K. & Wang S. 2019. Climate-driven trends of biogenic volatile organic compound emissions and their impacts on summertime ozone and secondary organic aerosol in China in the 2050s. *Atmospheric Environment* 218: 117020.

Luoma K., Niemi J.V., Aurela M., Fung P.L., Helin A., Hussein T., Kangas L., Kousa A., Rönkkö T., Timonen H., Virkkula A. & Petäjä T. 2021. Spatiotemporal variation and trends in equivalent black carbon in the Helsinki metropolitan area in Finland. *Atmospheric Chemistry and Physics* 21: 1173–1189.

Merikanto J., Spracklen D.V., Mann G.W., Pickering S.J. & Carslaw K.S. 2009. Impact of nucleation on global CCN. *Atmospheric Chemistry and Physics* 9: 8601–8616.

Mirme S. & Mirme A. 2013. The mathematical principles and design of the NAIS – a spectrometer for the measurement of cluster ion and nanometer aerosol size distributions. *Atmospheric Measurement Techniques* 6: 1061–1071.

Mohr C., Thornton J.A., Heitto A., Lopez-Hilfiker F.D., Lutz A., Riipinen I., Hong J., Donahue N.M., Hallquist M., Petäjä T., Kulmala M. & Yli-Juuti T. 2019. Molecular identification of organic vapors driving atmospheric nanoparticle growth. *Nature Communications* 10: 4442.

Nieminen T., Asmi A., Dal Maso M., Aalto P.P., Keronen P., Petaja T., Kulmala M. & Kerminen V.-M. 2014. Trends in atmospheric new-particle formation : 16 years of observations in a boreal-forest environment.

Patokoski J., Ruuskanen T.M., Hellén H., Taipale R., Gronholm T., Kajos M.K., Petaja T., Hakola H., Kulmala M. & Rinne J. 2014. Winter to spring transition and diurnal variation of VOCs in Finland at an urban background site and a rural site.

Peñuelas J. & Llusià J. 2003. BVOCs: plant defense against climate warming? *Trends in Plant Science* 8: 105–109.

Peñuelas J. & Staudt M. 2010. BVOCs and global change. *Trends in Plant Science* 15: 133–144.

Peräkylä O., Vogt M., Tikkanen O.-P., Laurila T., Kajos M.K., Rantala P.A., Patokoski J., Aalto J., Yli-Juuti T., Ehn M., Sipila M., Paasonen P., Rissanen M., Nieminen T., Taipale R., Keronen P., Lappalainen H.K., Ruuskanen T.M., Rinne J., Kerminen V.-M., Kulmala M., Back J. & Petaja T. 2014. Monoterpenes' oxidation capacity and rate over a boreal forest : temporal variation and connection to growth of newly formed particles.

Petäjä T., Mauldin I.I.I., Kosciuch E., McGrath J., Nieminen T., Paasonen P., Boy M., Adamov A., Kotiaho T. & Kulmala M. 2009. Sulfuric acid and OH concentrations in a boreal forest site. *Atmospheric Chemistry and Physics* 9: 7435–7448.

Rap A., Scott C.E., Spracklen D.V., Bellouin N., Forster P.M., Carslaw K.S., Schmidt A. & Mann G. 2013. Natural aerosol direct and indirect radiative effects. *Geophysical Research Letters* 40: 3297–3301.

Riccobono F., Schobesberger S., Scott C.E., Dommen J., Ortega I.K., Rondo L., Almeida J., Amorim A., Bianchi F., Breitenlechner M., David A., Downard A., Dunne E.M., Duplissy J., Ehrhart S., Flagan R.C., Franchin A., Hansel A., Junninen H., Kajos M., Keskinen H., Kupc A., Kürten A., Kvashin A.N., Laaksonen A., Lehtipalo K., Makhmutov V., Mathot S., Nieminen T., Onnela A., Petäjä T., Praplan A.P., Santos F.D., Schallhart S., Seinfeld J.H., Sipilä M., Spracklen D.V., Stozhkov Y., Stratmann F., Tomé A., Tsagkogeorgas G., Vaattovaara P., Viisanen Y., Vrtala A., Wagner P.E., Weingartner E., Wex H., Wimmer D., Carslaw K.S., Curtius J., Dona-

hue N.M., Kirkby J., Kulmala M., Worsnop D.R. & Baltensperger U. 2014. Oxidation Products of Biogenic Emissions Contribute to Nucleation of Atmospheric Particles. *Science* 344: 717–721.

Riipinen I., Yli-Juuti T., Pierce J.R., Petäjä T., Worsnop D.R., Kulmala M. & Donahue N.M. 2012. The contribution of organics to atmospheric nanoparticle growth. *Nature Geoscience* 5: 453–458.

Rinne J., Ruuskanen T.M., Reissell A., Taipale R., Hakola H. & Kulmala M. 2005. On-line PTR-MS measurements of atmospheric concentrations of volatile organic compounds in a European boreal forest ecosystem. *Boreal Environment Research* 10: 425–436.

Rogelj J., Rao S., McCollum D.L., Pachauri S., Klimont Z., Krey V. & Riahi K. 2014. Air-pollution emission ranges consistent with the representative concentration pathways. *Nature Climate Change* 4: 446–450.

Roldin P., Ehn M., Kurtén T., Olenius T., Rissanen M.P., Sarnela N., Elm J., Rantala P., Hao L., Hyttinen N., Heikkinen L., Worsnop D.R., Pichelstorfer L., Xavier C., Clusius P., Öström E., Petäjä T., Kulmala M., Vehkamäki H., Virtanen A., Riipinen I. & Boy M. 2019. The role of highly oxygenated organic molecules in the Boreal aerosol-cloud-climate system. *Nature Communications* 10: 4370.

Rose C., Zha Q., Dada L., Yan C., Lehtipalo K., Junninen H., Mazon S.B., Jokinen T., Sarnela N., Sipilä M., Petäjä T., Kerminen V.-M., Bianchi F. & Kulmala M. 2018. Observations of biogenic ion-induced cluster formation in the atmosphere. *Science Advances* 4: eaar5218.

Semenov V.A. 2012. Meteorology: Arctic warming favours extremes. *Nature Climate Change* 2: 315–316.

Sihto S.-L., Kulmala M., Kerminen V.-M., Dal Maso M., Petäjä T., Riipinen I., Korhonen H., Arnold F., Janson R., Boy M., Laaksonen A. & Lehtinen K.E.J. 2006. Atmospheric sulphuric acid and aerosol formation: implications from atmospheric measurements for nucleation and early growth mechanisms. *Atmospheric Chemistry and Physics* 6: 4079–4091.

Simon M., Dada L., Heinritzi M., Scholz W., Stolzenburg D., Fischer L., Wagner A.C., Kürten A., Rörup B., He X.-C., Almeida J., Baalbaki R., Baccarini A., Bauer P.S., Beck L., Bergen A., Bianchi F., Bräkling S., Brilke S., Caudillo L., Chen D., Chu B., Dias A., Draper D.C., Duplissy J., El-Haddad I., Finkenzeller H., Frege C., Gonzalez-Carracedo L., Gordon H., Granzin M., Hakala J., Hofbauer V., Hoyle C.R., Kim C., Kong W., Lamkaddam H., Lee C.P., Lehtipalo K., Leiminger M., Mai H., Manninen H.E., Marie G., Marten R., Mentler B., Molteni U., Nichman L., Nie W., Ojdanic A., Onnela A., Partoll E., Petäjä T., Pfeifer J., Philippov M., Quéléver L.L.J., Ranjithkumar A., Rissanen M.P., Schallhart S., Schobesberger S., Schuchmann S., Shen J., Sipilä M., Steiner G., Stozhkov Y., Tauber C., Tham Y.J., Tomé A.R., Vazquez-Pufleau M., Vogel A.L., Wagner R., Wang M., Wang D.S., Wang Y., Weber S.K., Wu Y., Xiao M., Yan C., Ye P., Ye Q., Zauner-Wieczorek M., Zhou X., Baltensperger U., Dommen J., Flagan R.C., Hansel A., Kulmala M., Volkamer R., Winkler P.M., Worsnop D.R., Donahue N.M., Kirkby J. & Curtius J. 2020. Molecular understanding of new-particle formation from α-pinene between −50 and +25 °C. *Atmospheric Chemistry and Physics* 20: 9183–9207.

Sipilä M., Berndt T., Petäjä T., Brus D., Vanhanen J., Stratmann F., Patokoski J., Mauldin R.L., Hyvärinen A.-P., Lihavainen H. & Kulmala M. 2010. The Role of Sulfuric Acid in Atmospheric Nucleation. *Science* 327: 1243–1246.

Spracklen D.V., Carslaw K.S., Merikanto J., Mann G.W., Reddington C.L., Pickering S., Ogren J.A., Andrews E., Baltensperger U., Weingartner E., Boy M., Kulmala M., Laakso L., Lihavainen H., Kivekäs N., Komppula M., Mihalopoulos N., Kouvarakis G., Jennings S.G., O'Dowd C., Birmili W., Wiedensohler A., Weller R., Gras J., Laj P., Sellegri K., Bonn B., Krejci R., Laaksonen A., Hamed A., Minikin A., Harrison R.M., Talbot R. & Sun J. 2010. Explaining global surface aerosol number concentrations in terms of primary emissions and particle formation. *Atmospheric Chemistry and Physics* 10: 4775–4793.

Stolzenburg, D., Cai, R., Blichner, S. M., Kontkanen, J., Zhou, P., Makkonen, R., Kerminen, V-M., Kulmala, M., Riipinen, I. and Kangasluoma, J.: Atmospheric nanoparticle growth, Reviews of Modern Physics. 2023 Taipale R., Ruuskanen T.M., Rinne J., Kajos M.K., Hakola H., Pohja T. & Kulmala M. 2008. Technical Note: Quantitative long-term measurements of VOC concentrations by PTR-MS – measurement, calibration, and volume mixing ratio calculation methods. *Atmospheric Chemistry and Physics* 8: 6681–6698.

Taipale R., Ruuskanen T.M., Rinne J., Kajos M.K., Hakola H., Pohja T. & Kulmala M. 2008. Technical Note: Quantitative long-term measurements of VOC concentrations by PTR-MS – measurement, calibration, and volume mixing ratio calculation methods. Atmospheric Chemistry and Physics 8: 6681–6698.

Tarvainen V., Hakola H., Hellén H., Bäck J., Hari P. & Kulmala M. 2005. Temperature and light dependence of the VOC emissions of Scots pine. *Atmospheric Chemistry and Physics* 5: 989–998.

Tröstl J., Herrmann E., Frege C., Bianchi F., Molteni U., Bukowiecki N., Hoyle C.R., Steinbacher M., Weingartner E., Dommen J., Gysel M. & Baltensperger U. 2016. Contribution of new particle formation to the total aerosol concentration at the high-altitude site Jungfraujoch (3580 m asl, Switzerland). *Journal of Geophysical Research: Atmospheres* 121: 11,692-11,711.

Valolahti H., Kivimäenpää M., Faubert P., Michelsen A. & Rinnan R. 2015. Climate change-induced vegetation change as a driver of increased subarctic biogenic volatile organic compound emissions. *Global Change Biology* 21: 3478–3488.

Wang J., Taylor A.R. & D'Orangeville L. 2023. Warming-induced tree growth may help offset increasing disturbance across the Canadian boreal forest. *Proceedings of the National Academy of Sciences* 120: e2212780120.

Weber R.J., Marti J.J., McMurry P.H., Eisele F.L., Tanner D.J. & Jefferson A. 1996. Measured Atmospheric New

Particle Formation Rates: Implications for Nucleation Mechanisms. *Chemical Engineering Communications* 151: 53–64.

Wiedinmyer C., Tie X., Guenther A., Neilson R. & Granier C. 2006. Future Changes in Biogenic Isoprene Emissions: How Might They Affect Regional and Global Atmospheric Chemistry? *Earth Interactions* 10: 1–19.

Xu Y., Zhou B.-T., Wu J., Han Z.-Y., Zhang Y.-X. & Wu J. 2017. Asian climate change under 1.5–4 °C warming targets. *Advances in Climate Change Research* 2: 99–107.

Yan C., Dada L., Rose C., Jokinen T., Nie W., Schobesberger S., Junninen H., Lehtipalo K., Sarnela N., Makkonen U., Garmash O., Wang Y., Zha Q., Paasonen P., Bianchi F., Sipilä M., Ehn M., Petäjä T., Kerminen V.-M., Worsnop D.R. & Kulmala M. 2018. The role of H_2SO_4-NH_3 anion clusters in ion-induced aerosol nucleation mechanisms in the boreal forest. *Atmospheric Chemistry and Physics* 18: 13231–13243.

Yan C., Nie W., Vogel A.L., Dada L., Lehtipalo K., Stolzenburg D., Wagner R., Rissanen M.P., Xiao M., Ahonen L., Fischer L., Rose C., Bianchi F., Gordon H., Simon M., Heinritzi M., Garmash O., Roldin P., Dias A., Ye P., Hofbauer V., Amorim A., Bauer P.S., Bergen A., Bernhammer A.-K., Breitenlechner M., Brilke S., Buchholz A., Mazon S.B., Canagaratna M.R., Chen X., Ding A., Dommen J., Draper D.C., Duplissy J., Frege C., Heyn C., Guida R., Hakala J., Heikkinen L., Hoyle C.R., Jokinen T., Kangasluoma J., Kirkby J., Kontkanen J., Kürten A., Lawler M.J., Mai H., Mathot S., Mauldin R.L., Molteni U., Nichman L., Nieminen T., Nowak J., Ojdanic A., Onnela A., Pajunoja A., Petäjä T., Piel F., Quéléver L.L.J., Sarnela N., Schallhart S., Sengupta K., Sipilä M., Tomé A., Tröstl J., Väisänen O., Wagner A.C., Ylisirniö A., Zha Q., Baltensperger U., Carslaw K.S., Curtius J., Flagan R.C., Hansel A., Riipinen I., Smith J.N., Virtanen A., Winkler P.M., Donahue N.M., Kerminen V.-M., Kulmala M., Ehn M. & Worsnop D.R. 2020. Size-dependent influence of NOx on the growth rates of organic aerosol particles. *Science Advances* 6: eaay4945.

Yan C., Yin R., Lu Y., Dada L., Yang D., Fu Y., Kontkanen J., Deng C., Garmash O., Ruan J., Baalbaki R., Schervish M., Cai R., Bloss M., Chan T., Chen T., Chen Q., Chen X., Chen Y., Chu B., Dällenbach K., Foreback B., He X., Heikkinen L., Jokinen T., Junninen H., Kangasluoma J., Kokkonen T., Kurppa M., Lehtipalo K., Li H., Li H., Li X., Liu Y., Ma Q., Paasonen P., Rantala P., Pileci R.E., Rusanen A., Sarnela N., Simonen P., Wang S., Wang W., Wang Y., Xue M., Yang G., Yao L., Zhou Y., Kujansuu J., Petäjä T., Nie W., Ma Y., Ge M., He H., Donahue N.M., Worsnop D.R., Kerminen V.-M., Wang L., Liu Y., Zheng J., Kulmala M., Jiang J. & Bianchi F. 2021. The Synergistic Role of Sulfuric Acid, Bases, and Oxidized Organics Governing New-Particle Formation in Beijing. *Geophysical Research Letters* 48: e2020GL091944.

Yao L., Garmash O., Bianchi F., Zheng J., Yan C., Kontkanen J., Junninen H., Mazon S.B., Ehn M., Paasonen P., Sipilä M., Wang M., Wang X., Xiao S., Chen H., Lu Y., Zhang B., Wang D., Fu Q., Geng F., Li L., Wang H., Qiao L., Yang X., Chen J., Kerminen V.-M., Petäjä T., Worsnop D.R., Kulmala M. & Wang L. 2018. Atmospheric new particle formation from sulfuric acid and amines in a Chinese megacity. *Science* 361: 278–281.

Zhang R., Suh I., Zhao J., Zhang D., Fortner E.C., Tie X., Molina L.T. & Molina M.J. 2004. Atmospheric New Particle Formation Enhanced by Organic Acids. *Science* 304: 1487–1490.

Zhao D.F., Buchholz A., Tillmann R., Kleist E., Wu C., Rubach F., Kiendler-Scharr A., Rudich Y., Wildt J. & Mentel T.F. 2017. Environmental conditions regulate the impact of plants on cloud formation. *Nature Communications* 8: 14067.